

Accurate on line measurements of low fluences of charged particles

L. Palla^{1,2}, C. Czelusniak^{3,4}, F. Taccetti³, L. Carraresi^{3,4,a}, L. Castelli³, M.E. Fedi³, L. Giuntini^{3,4}, P.R. Maurenzig^{4,b}, L. Sottili⁴, and N. Taccetti^{4,c}

¹ INFN, Sezione di Pisa, Largo B. Pontecorvo 3, 56127 Pisa, Italia

² Dipartimento di Fisica, Università di Pisa, Largo Bruno Pontecorvo 3, 56127 Pisa, Italia

³ INFN, Sezione di Firenze, Via Sansone 1, 50019 Sesto Fiorentino (FI), Italia

⁴ Dipartimento di Fisica e Astronomia, Università di Firenze, via Sansone 1, 50019 Sesto Fiorentino (FI), Italia

Received: 2 December 2014 / Revised: 15 January 2015

Published online: 6 March 2015 – © Società Italiana di Fisica / Springer-Verlag 2015

Abstract. Ion beams supplied by the 3 MV Tandem accelerator of LABEC laboratory (INFN-Firenze), have been used to study the feasibility of irradiating materials with ion fluences reproducible to about 1%. Test measurements have been made with 7.5 MeV ${}^7\text{Li}^{2+}$ beams of different intensities. The fluence control is based on counting ions contained in short bursts generated by chopping the continuous beam with an electrostatic deflector followed by a couple of adjustable slits. Ions are counted by means of a micro-channel plate (MCP) detecting the electrons emitted from a thin layer of Al inserted along the beam path in between the pulse defining slits and the target. Calibration of the MCP electron detector is obtained by comparison with the response of a Si detector.

1 Introduction

The thermoluminescence of materials such as quartz, amorphous silica and feldspars has been used for a long time to measure ionizing radiation dose in different fields such as environmental dosimetry [1], dosimetry of radio-therapeutic beams [2] and, more recently, in archaeometry, in most cases for dating purposes [3]¹. The refinement of these measurements demands more and more accurate calibrations of the dosimeters: to this aim a lot of measurements have been performed with different kinds of radiations at different energies and with different fluences [4, 5]; also possible dose rate effects have been investigated [6]. In this framework the present paper reports a preliminary study on the feasibility of irradiating materials with total fluences in the range (10^5 – 10^{11}) cm^{-2} measured on line with a precision of the order of 1%.

In sect. 2 the irradiation technique, based on a pulsed beam, is briefly described. In sect. 3 the measure of the fluence by means of a MCP which detects the electrons emitted from a layer of Al placed on the beam path is presented together with the calibration of the Al layer plus MCP assembly by comparing its response with that of a Si detector. In sect. 4 a set of measurements performed with a beam intensity variation of about 35% is presented. Some comments about very preliminary measurements of smaller statistics with oxygen and proton beams are also reported.

2 Main features of the experimental set-up

The irradiation technique makes use of ion bursts generated by the transitions of an electrostatic deflector (DEFEL in the following) installed in a beam line of the Tandem of LABEC [7,8]. Following the voltage transitions of the deflector, only for short time intervals a small number of ions passes through an adjustable aperture placed downstream and

^a e-mail: carraresi@fi.infn.it

^b Retired.

^c Retired.

¹ As is well known, the thermoluminescence of quartz is widely used for dating inorganic samples of ages from less than 100 to 250000 years. Since the average absorbed dose due to α particles of the natural series of U and Th (rough mean energy 4 MeV) is about 2 mGy per year [3], the quoted range of dating corresponds to average doses between (0.2 and 500) Gy. Referring to a volume of $1\text{ cm} \times 1\text{ cm} \times 15\text{ }\mu\text{m}$ (range of α particles) one needs fluences in the range 10^6 – 10^9 cm^{-2} .

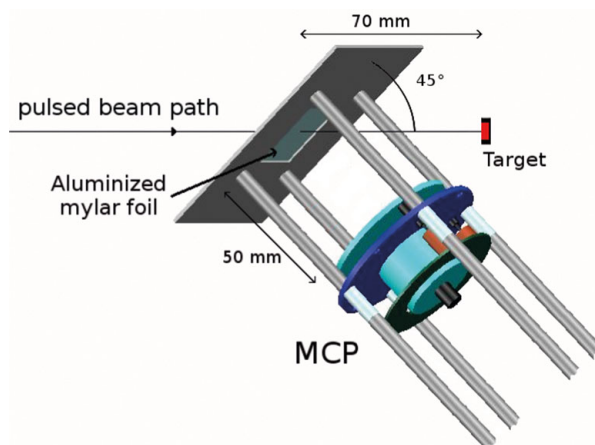


Fig. 1. Experimental setup. The MCP detector assembly can be moved vertically from the measurement position to another one not interfering with the beam path. For calibration and test measurements a Si detector can be moved to replace the target.

hits the target. Targets are mounted inside a vacuum chamber on a frame movable along the x and y axes, the z -axis being the beam path. Step motors drive the (x, y) displacements (± 20 cm) with a reproducibility within few microns. The operation and the performance of DEFEL are presented in details in refs. [9, 10]. Here, only the characteristics of interest for the present application are recalled: 1) the pulse repetition frequency can be chosen from single shot up to 10 kHz; 2) the mean number of ions per burst (μ) can be varied from < 1 up to many hundreds; 3) the duration of the bursts (FW1/10M) is typically in the range (0.5–5.0) ns; 4) the area of the beam on target can be set from $100 \mu\text{m} \times 100 \mu\text{m}$ up to $3 \text{mm} \times 3 \text{mm}$; 5) for a steady beam current the number of ions per burst follows the Poisson statistics.

In case of constant beam current that generates bursts of a mean value μ of ions per burst, the simplest procedure for irradiating a sample with a precise fluence makes use of a previous irradiation of a Si detector. In fact, because of its good energy resolution, the Si detector shows well separated peaks corresponding to bursts of different ion multiplicity m so that a precise counting of the ion number impinging on the detector is easily obtained. In practice, first the Si detector is irradiated with a predetermined number of bursts, afterwards the sample is irradiated with the planned number of bursts and the fluence is obtained by a simple scaling procedure. However, also in case of modest fluences, the irradiation time could be so long that a beam current stability better than 1% cannot be guaranteed, so it seems useful to devise a technique for measuring the fluence during the irradiation.

As shown in fig. 1, the measurement of the fluence relies on the presence of a foil centred on the beam axis at a distance of 70 mm before the target, and tilted at an angle of 45° . This foil consists of a $1.5 \mu\text{m}$ supporting mylar foil with a 20 nm Al layer deposited on the side facing the MCP. Ions passing through the Al layer release electrons which are detected by a 2-stages MCP² whose input electrode is at a distance of 50 mm from the foil and parallel to it. The assembly of the Al layer plus MCP constitutes the electron detector which, for short, in the following will be referred to as MCP detector. This assembly is mounted on a pantograph which can be moved by a step motor along the vertical axis. In this way, before a calibration measurement, the foil can be removed from the beam path and the Si detector can record the spectrum of bursts impinging directly on it. The comparison of this spectrum with that recorded in the presence of the foil makes it possible to measure the energy loss of the ions traversing the foil from the difference in peak positions. In this way the final energy E_f of 7.5 MeV ${}^7\text{Li}^{2+}$ ions was measured to be (6.67 ± 0.02) MeV.

It should be emphasized that also the calibration of the MCP detector takes advantage of the energy resolution of the Si detector, which makes it possible both an easy counting of ion bursts passed through the foil and a precise measurement of their energies (that means ion multiplicities). Concerning the MCP detector, the voltage accelerating electrons emitted by the foil toward the grounded MCP input electrode, was set to -500 V, while the standard voltage distribution was used for biasing the MCP: 1 kV per stage and 400 V between anode and MCP output electrode.

3 MCP detector calibration

As already said, the calibration is made by comparing the response of the MCP detector with that of a Si detector³ placed at the target location. A typical measurement run consists of a predetermined number of DEFEL triggers starting the acquisition of a digitizer⁴ that samples the anode pulses of the MCP (FWHM of about 5–6 ns after the

² Hamamatsu mod. F4655-12: effective area $\simeq 1.65 \text{cm}^2$, gain (at 2.4 kV) $\simeq 5.10^7$, resolution 50%.

³ Hamamatsu mod. S3590-04: effective area 1cm^2 , thickness $300 \mu\text{m}$, no window.

⁴ CAEN mod. V1720: 8 channels (single-ended input), range ± 1000 mV, offset ± 1000 mV, input filter bandwidth 125 MHz, resolution 12 bit (10.5 enob), sampling rate 250 MS/s, memory 1.25 MS/ch.

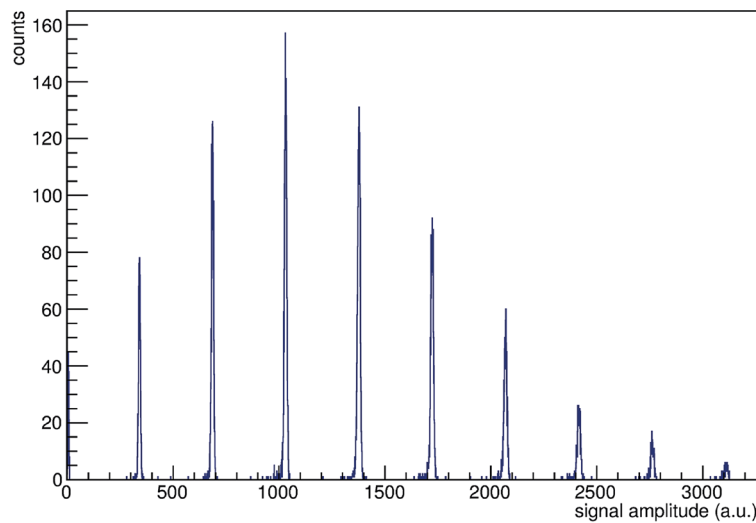


Fig. 2. Amplitude spectrum of the Si detector showing peaks with ion multiplicity $m = 1, \dots, 9$.

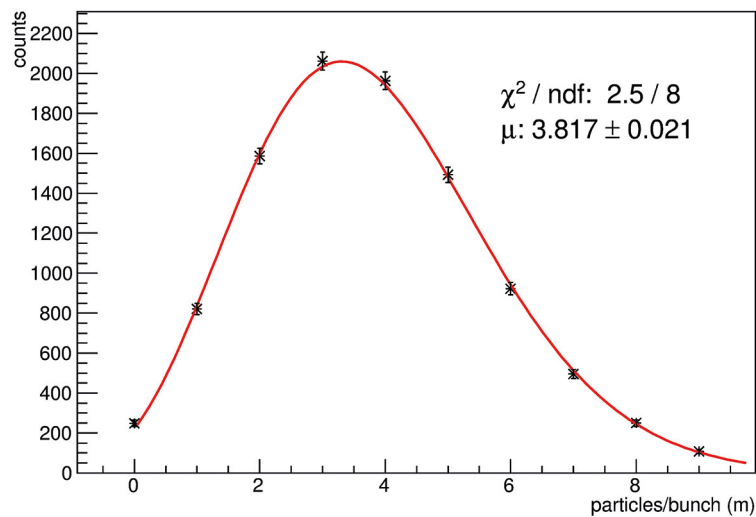


Fig. 3. Poissonian fit of the ions number distribution in the peaks of fig. 2.

digitizer) and the coincident output signals of the Si detector processed by a charge preamplifier followed by a semi-gaussian amplifier (shaping time $0.5 \mu\text{s}$). The couples of digitized waveforms compose the events which are stored in a mass memory for off-line analysis. Each single acquisition lasts $32 \mu\text{s}$ (8000 samples), the first $14 \mu\text{s}$ being used for baseline evaluation.

Figure 2 shows the Si detector spectrum of the calibration measurement, which was the first one of a set of 5 test measurements presented in detail in the following. The spectrum, corresponding to 10000 trigger signals, was obtained by applying a numerical integration in an interval of $1.2 \mu\text{s}$ (300 samples) centred around the peak of the shaped signal.

Moreover, as shown in fig. 3, the number of counts per peak (every peak corresponding to a given multiplicity m , that means to an integer number of ions per burst) follows a Poisson distribution with a mean value $\mu_{Si} = 3.817 \pm 0.021$ ions per burst. In agreement with the Poisson distribution, about 240 events with no ions are observed.

In fig. 4(a) the corresponding amplitude spectrum obtained from the anode signals of the MCP detector is reported. A numerical integration was applied also to these signals: in this case the integration time from the beginning of the signal lasted 100 ns (25 samples). At variance with the Si detector spectrum, this one does not show resolved peaks of well-defined amplitude (*i.e.* number of ions) mainly because of the small number of electrons per ion emitted by the Al layer and also of the poor resolution of the MCP. However, the unresolved components of different multiplicity contributing to the spectrum can be easily singled out by means of their coincidence with the corresponding signals of the Si detector. Part (b) of fig. 4 shows the amplitude distributions of some of these components.

Other four test measurements, made with μ_{Si} mean values ranging from 3.777 to 5.070, show that the mean B_m of the amplitude distribution corresponding to the multiplicity m is independent of μ_{Si} . So the mean B_T of any total spectrum of mean multiplicity μ can be written down as $B_T = \sum_m W_m(\mu) B_m$ where the weight W_m is given by the

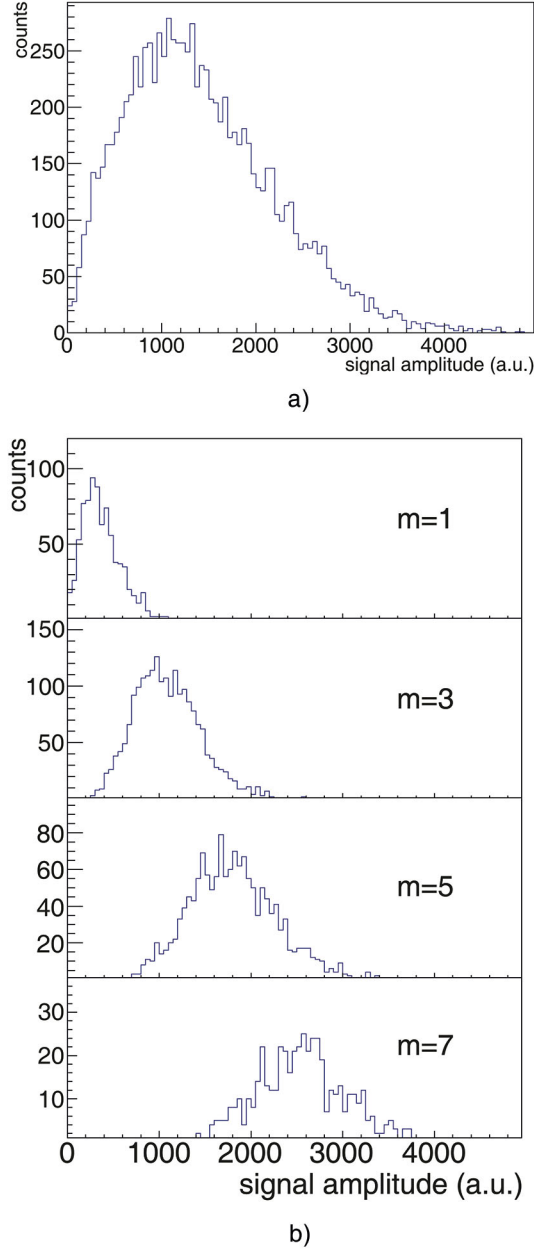


Fig. 4. (a) Total amplitude spectrum of the MCP detector: no peaks are apparent. (b) As an example the amplitude distributions of the components of multiplicity 1, 3, 5, 7 are shown.

integral of the corresponding distribution (see fig. 4(b)). These integrals coincide, within the statistical errors, with the Poissonian weights.

The calibration procedure is based on the construction of the MCP detector amplitude distributions, corresponding to mean values μ of ions per burst ranging from 0.5 to 5.0 (step 0.5). For any selected μ value, the number of events expected for each multiplicity is given by the Poisson statistics and its amplitude distribution is taken from the distributions of fig. 4(b). The weighted sum of the amplitude distributions of all multiplicities (with non vanishing number of events) gives the expected total spectrum of the MCP detector for the considered μ value. As shown in fig. 5, the mean values B_T of these total amplitude spectra, taking into account also the events with no ions, come out to be in linear relationship with the μ values: $B_T = K\mu$. This establishes the calibration of the MCP detector. It should be observed that the K factor depends on several factors: the electron yield of the Al foil and, therefore, the ion type and its stopping power (K_{foil}), the MCP and its applied voltage (K_{MCP}), the attenuation and bandwidth limit in the transmission of signals to the digitizer (K_{el}), the conversion gain of the digitizer (K_D) and the software treatment of the digitized signals (K_{soft}), that means

$$K = K_{foil}K_{MCP}K_{el}K_DK_{soft}. \quad (1)$$

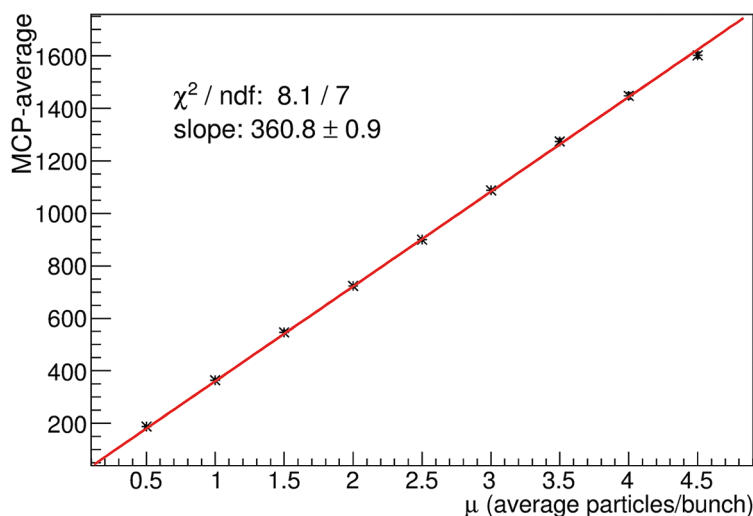


Fig. 5. Relationship among mean values B_T of the calculated energy spectra of the MCP detector and mean values μ (see text).

This factor is a constant depending only on the chosen operating conditions.

In a true measurement, after calibration, each sample is irradiated with bursts from N triggers and, at the same time, the amplitude spectrum of the MCP detector is collected. By entering the mean of this spectrum in fig. 5, the associated μ value is found and the fluence is given by $N\mu$.

Moreover, a measurement during which the beam current (and consequently the mean value μ) changes appreciably may be interpreted as the sum of shorter measurements, each with a well defined mean value. As a consequence, the calibrated MCP detector, which gives a real time response even in case of “rapidly” changing μ values, makes it possible to correctly measure the fluence rate and the total fluence. As a matter of fact, this means that for a given ion-beam of determined energy, and for a given K factor, after calibration, it is possible to calculate the fluence deposited on the sample, as the product of the mean value μ from B_T of the measured spectrum and the number of triggers selected in the run. The corresponding dose can then be obtained after measuring the energy loss of the ions inside the foil. It is worth to stress that this result is strictly related to the 100% efficiency of the MCP detector and that all the recorded blank events are of Poissonian origin.

4 Results and discussion

As a check, the procedure was applied to 4 runs, each of 10^4 triggers, taken after the run used to construct the calibration curve of fig. 5. The results are presented in table 1. Columns 3 and 4 show a nice agreement among μ values derived from B_T (column 2) by means of the calibration curve taken from run 1 and μ_{Si} values directly measured by the Si detector. The largest difference comes out for the run 2, but it is still better than 1%, as it can be seen from the last column. In each run the average dose delivered to the Si detector (within the beam spot size of about $1\text{ mm} \times 1.5\text{ mm}$) was in the range (790–1050) mGy.

Table 1. Mean values of the ion number per burst obtained from the B_T value and the calibration curve of MCP detector, compared with the value given by the Si detector.

Run number	B_T	μ_{MCP}	μ_{Si}	$[\mu_{MCP} - \mu_{Si}]/\mu_{Si}$
1	1381 ± 8	3.823 ± 0.024	3.817 ± 0.021	+0.16%
2	1374 ± 8	3.808 ± 0.024	3.777 ± 0.021	+0.82%
3	1619 ± 9	4.487 ± 0.027	4.497 ± 0.024	-0.22%
4	1820 ± 9	5.044 ± 0.028	5.070 ± 0.026	-0.51%
5	1726 ± 9	4.784 ± 0.025	4.785 ± 0.025	-0.02%

Here we can prove that the method works also in case of beam current variations or beam instabilities. During each of the 5 runs the beam current was substantially stable, but it differed in the different runs. We can consider runs 2, 3, 4, 5 as a unique longer run during which the current changed of about 35% throughout the measurement. For this unique run we obtain $\mu_{Si} = 4.532 \pm 0.013$ and $\mu_{MCP} = 4.533 \pm 0.024$.

An agreement similar to that obtained with the lithium ions has been found in a series of measurements performed with a 10 MeV beam of $^{16}\text{O}^{4+}$: in particular a 100% detection efficiency of the MCP detector was again found. The calibration curve for $^{16}\text{O}^{4+}$ is a linear function as in the case of $^7\text{Li}^{2+}$, with a χ^2/ndf of 7.5/8 and a slope of 376 ± 3 .

Measurements with ^4He beams, directly usable *e.g.* for calibration of archaeometry studies, were planned but postponed to a future run after the planned upgrading of the source of the Tandem. A preliminary series of measurements with 1 MeV proton beam put in evidence that the detection efficiency is in this case smaller than 100% up to burst of multiplicity $m \simeq 5$. In these conditions, the calibration procedure discussed in sect. 3 must be modified to take into account the undetected ions.

5 Conclusions

This work suggests the feasibility of precise measurements of fluence also in the presence of large fluctuations of the beam current. In irradiation measurements with quartz samples or with other kinds of target materials the system is expected to provide the chosen dose with high accuracy. New series of test measurements will be carried out with different ion species, especially with protons, in order to test the method under critical conditions and to optimize the calibration procedure also for this case. Besides, as the method allows a simultaneous measurement of the dose during the irradiation, the system will be upgraded in order to monitor the MCP integral spectra and to evaluate on-line the corresponding mean. This will allow to compensate for possible fluctuations in the average multiplicity of the bunches by increasing or decreasing the duration of the measurement.

The authors would like to warmly thank Dr. A. Olmi for the critical reading of the manuscript and M. Manetti for his valuable technical collaboration.

References

1. M. Nikolae, K. Turkush, in *Problems of radiation safety provisions at nuclear power plants operation*, Vol. 2 (1976) p. 142.
2. J.R. Cameron, F. Daniels, N. Johnson, G. Kinney, *Science* **134**, 333 (1961).
3. M.J. Aitken, *Thermoluminescence Dating* (Academic Press, London, 1985).
4. M.E. Brandan, I. Gamboa-deBuen, M. Rodríguez-Villafuerte, *Radiat. Prot. Dosim.* **100**, 39 (2002).
5. E.G. Yukihara, R. Gazaa, S.W.S. McKeever, C.G. Soares, *Radiat. Meas.* **38**, 59 (2004).
6. S. Chawla, T.K. Gundu Rao, A.K. Singhvi, *Radiat. Meas.* **29**, 53 (1998).
7. P.A. Mandò, *Il Nuovo Cimento C* **30**, 85 (2007).
8. <http://labec.fi.infn.it/>.
9. F.A. Mirto, L. Carraresi, *Nucl. Instrum. Methods Phys. Res. B* **266**, 2113 (2010).
10. N. Taccetti, L. Giuntini, G. Casini, A.A. Stefanini, M. Chiari, M.E. Fedi, P.A. Mandò, *Nucl. Instrum. Methods Phys. Res. B* **188**, 255 (2002).